# PROCEEDINGS OF SPIE

SPIEDigitalLibrary.org/conference-proceedings-of-spie

# Four-dimensional optoacoustic temperature mapping in laser-induced thermotherapy

Francisco Javier Oyaga Landa, Xosé Luís Deán-Ben, Ronald Sroka, Daniel Razansky

Francisco Javier Oyaga Landa, Xosé Luís Deán-Ben, Ronald Sroka, Daniel Razansky, "Four-dimensional optoacoustic temperature mapping in laser-induced thermotherapy," Proc. SPIE 10494, Photons Plus Ultrasound: Imaging and Sensing 2018, 104940D (19 February 2018); doi: 10.1117/12.2288924



Event: SPIE BiOS, 2018, San Francisco, California, United States

# Four-dimensional optoacoustic temperature mapping in laser-induced thermotherapy

Francisco Javier Oyaga Landa,  $^{1,2}$  Xosé Luís Deán-Ben,  $^1$  Ronald Sroka,  $^3$  and Daniel Razansky  $^{1,2,\,*}$ 

<sup>1</sup>Institute for Biological and Medical Imaging (IBMI), Helmholtz Zentrum München, Neuherberg, Germany

<sup>2</sup>School of Medicine, Technische Universität München (TUM), Munich, Germany
<sup>3</sup>Laser Research Laboratory/LIFE Center, Ludwig-Maximilian-University, Munich, Germany
\*Corresponding author: dr@tum.de

### ABSTRACT

Photoablative laser therapy is in common use for selective destruction of malignant masses, vascular and brain abnormalities. Tissue ablation and coagulation are irreversible processes occurring shortly after crossing a certain thermal exposure threshold. As a result, accurate mapping of the temperature field is essential for optimizing the outcome of these clinical interventions. Here we demonstrate four-dimensional optoacoustic temperature mapping of the entire photoablated region. Accuracy of the method is investigated in tissue-mimicking phantom experiments. Deviations of the volumetric optoacoustic temperature readings provided at 40ms intervals remained below 10% for temperature elevations above 3°C, as validated by simultaneous thermocouple measurements. The excellent spatio-temporal resolution of the new temperature monitoring approach aims at improving safety and efficacy of laser-based photothermal procedures.

**Keywords:** Ablation of Tissue; Optoacoustic Tomography; Temperature; Thermal Treatments.

## 1. INTRODUCTION

Thermal ablation procedures are widely employed in clinical interventions such as in selective ablation of cancerous tissues, benign hyperplasias or varicose veins as well as in the treatment of cardiac arrhythmias and enhanced drug delivery. Thermal ablation procedures can be classified depending on the heat source used. Laser light, focused ultrasound, radio-frequency current and microwaves are commonly employed. Laser-induced thermotherapy (LITT), also known as laser ablation, has gained popularity due to its advantages, such as reduced treatment times, minimal invasiveness and low hardware investment. LITT is carried out employing laser radiation as energy source, usually guided through optic fibers.

Heat-driven denaturation generally takes place when tissues are heated above 50°C, while the exposure time further determines the size of the induced lesion. Therefore, the spatio-temporal temperature distribution in the treated tissue plays a crucial role in the outcome of photothermal interventions. On the other hand, several therapeutic procedures use lower temperature elevations without inducing irreversible tissue damage, including local and whole-body hyperthermia<sup>5</sup> as well as low- and medium-intensity focused ultrasound.<sup>6,7</sup> The effectiveness of thermal therapies heavily relies on the ability to accurately monitor and control the volumetric temperature distribution of the treated tissues in real time.<sup>2</sup> Optoacoutic signals are very sensitive to temperature changes.<sup>8,9</sup> Previous works have established the dependence of the optoacoustic signal during thermal therapies. This has been exploited for non-invasive temperature monitoring in clinical procedures involving radiofrequency ablation,<sup>10</sup> high-intensity focused ultrasound (HIFU),<sup>11</sup> cryoablation<sup>12</sup> or laser-induced thermotherapy (LITT).<sup>13,14</sup> Herein, we describe an approach for optoacoustic monitoring of photothermal therapy that offers high sensitivity to temperature fluctuations.<sup>14</sup> The performance of optoacoutics to dynamically map temperature in a three-dimensional volume is showcased.

Photons Plus Ultrasound: Imaging and Sensing 2018, edited by Alexander A. Oraevsky, Lihong V. Wang, Proc. of SPIE Vol. 10494, 104940D · © 2018 SPIE · CCC code: 1605-7422/18/\$18 · doi: 10.1117/12.2288924

#### 2. METHODS

# 2.1 Optoacoustic Image Acquisition Set-up and Reconstruction

The lay-out of the experimental setup is depicted in Figure 1. Dynamic volumetric temperature monitoring was performed with a three-dimensional optoacoustic probe made of a 512-element spherical transducer array covering an angle of 140° with 4 cm radius of curvature  $(1.3\pi \text{ solid angle})$ . The individual elements of the array have a central frequency of 5 MHz and 100% detection bandwidth, corresponding to nearly isotropic imaging resolution of 150  $\mu$ m around the geometrical center of the sphere. Acoustic coupling was ensured by molding agarose gel between the active surface and the surface of the imaged sample (Figure 1). Optoacoustic responses were excited with a short-pulsed (<10 ns) laser source (Innolas Laser GmbH, Krailling, Germany) guided via a custom-made fiber bundle (CeramOptec GmbH, Bonn, Germany) through a hollow cylindrical cavity in the center of the array. For imaging, the wavelength of the tunable optoacoustic laser source was also set to 830 nm and the optical fluence was roughly  $11 \text{ mJ}/\text{cm}^2$  at the surface of the imaged sample. The pulse repetition frequency (PRF) of the laser was set to 5 Hz. A second arm of the fiber bundle was guided to a powermeter (EM-USB-J-25MB-LE, Coherent Inc., Santa Clara, California) to monitor the energy per pulse, which was used to normalize the acquired signals. All 512 OA signals were simultaneously digitized at 40 mega-samples per second (MSPS) by a custom-made data acquisition (DAQ) system (Falkenstein Mikrosysteme GmbH, Taufkirchen, Germany) triggered with the Q-switch output of the laser. The acquired signals were deconvolved with the impulse response of the array elements and band-pass filtered between 0.1MHz and 7MHz, and a graphics processing unit (GPU)-based 3D back-projection algorithm was used for tomographic reconstruction. <sup>15</sup> The ablation fiber heated the tissue through a diode laser providing 20W of continuous wave power at 830 nm (Indigo 830, Indigo Medical Inc., Lawrenceville, New Jersey). A specialized fiberoptic delivery system with a cylindrical diffuser at the tip was used to guide the ablation beam to the region of interest.

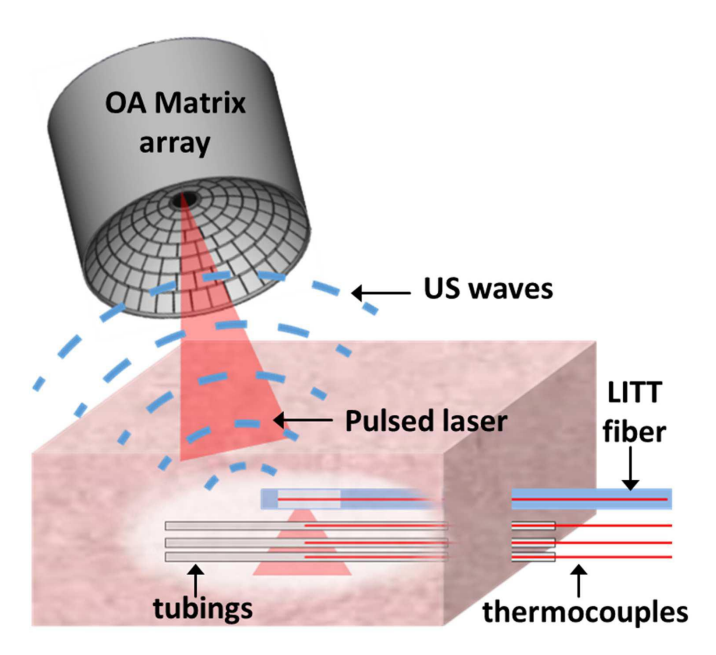


Figure 1. (a) Lay-out of the experimental setup. The tissue mimicking phantom is excited by a pulsed laser light guided through the axial cavity of the transducer array for the generation of optoacoustic responses. On the other hand, the CW laser heats the absorving murine blood chromophores found in the embedded tubings. The temperature at three known locations within the tubings was tracked with thermocouples.

# 2.2 Temperature Estimation Method

The suggested optoacoustic temperature estimation method relays on the temperature dependence of the optoacoustic signals. Stress confinement can be assumed when the optoacoustic response are excited with a short-

duration laser pulse.<sup>16</sup> Under these conditions, the initial OA pressure wave is given by  $p_0 = \Gamma \mu_a \phi$ , being  $\Gamma$  the (dimensionless) Grüneisen parameter,  $\mu_a$  the optical absorption coefficient and  $\phi$  the light fluence. The temperature dependance of the generated OA signals mainly comes from variations in the Grüneisen parameter. In the water-like aqueous media, these variations can be approximated by <sup>16</sup>

$$\Gamma(T) = 0.0043 + 0.0053T. \tag{1}$$

where T is expressed in  $^{\circ}$ C. The relative change of the OA signal as a function of the temperature increase  $\Delta$ T can be then expressed as

$$\frac{\Delta p_0}{p_{0.0}} = \frac{0.0053\Delta T}{0.0043 + 0.0053 \cdot T_0} \tag{2}$$

being  $p_{0,0}$  and  $T_0$  the initial (baseline) optoacoustic signal and the initial temperature before the ablation experiment, respectively. According to Eq. 2, the amplitude of the OA signals is expected to increase by approximately 2.7% per degree for typical temperature values of 36°C in living organisms. We further define F as the ratio between the relative increment of the OA signal and the relative increment of temperature, i.e.,

$$F = \frac{T_0}{p_{0,0}\Delta T} \Delta p_0 \tag{3}$$

Considering Eq. 2, the theoretical value of F(Fth) can be expressed as a function of the initial temperature  $T_0$  via

$$F_{th} = \left(\frac{0.8113}{T_0} + 1\right)^{-1} \tag{4}$$

The temperature increment can then be retrieved from the relative OA signal increase as

$$\Delta T = \frac{T_0}{p_{0.0}F} \Delta p_0 \tag{5}$$

Note that for temperatures above 50°C, the coagulation threshold, cell denaturation mechanisms are known to take place in soft biological tissues, which induce variations in the optical absorption and scattering coefficients of the ablated tissues.<sup>17</sup> Accuracy of the above temperature estimation method is thus expected to be limited to temperatures below the coagulation threshold.

#### 2.3 Phantom validation experiments

The temperature monitoring approach based on Eq. 5 was tested in a tissue-mimicking phantom. In this experiment, three tubings with 1 mm diameter and 10 mm length were embedded in a  $\sim$  8 mm layer of chicken breast. The tubings were filled with murine blood and sealed with glue. Three thermocouples (Physitemp Instruments Inc., Clifton, New Jersey) were inserted into the tubings to provide real-time temperature values. The thermocouple readings were digitized with an embedded NI 9213 DAQ (National Instruments Corporation, Austin, Texas, U.S.). For each tubing, the temperature estimations were retrieved from the values of the reconstructed optoacoustic images at the regions of interest (ROIs) corresponding to the locations of the thermocouple sensors.

## 3. RESULTS AND DISCUSSION

Figure 2 shows the reconstructed optoacoustic images at three different instants during the laser heating process. The ablation fiber was positioned parallel to the tubings at 5 mm from the leftmost one. The progressive increment in the optoacoustic signal as temperature increases can be perceived in all tubings (Figures 2a-c). The temperature increase in murine blood was then obtained from Eq. 5, where the F factor was calculated via Eq. 4. The estimated temperature increase inside the three tubings is plotted in Figure 2d as dashed lines. For calculating the relative signal increments, the baseline optoacoustic image was taken as the average of 50 frames before the ablation procedure. The reference temperature increase values, taken from readings from the thermocouples located at the same ROIs, are also shown in Figure 2d as continuous lines.

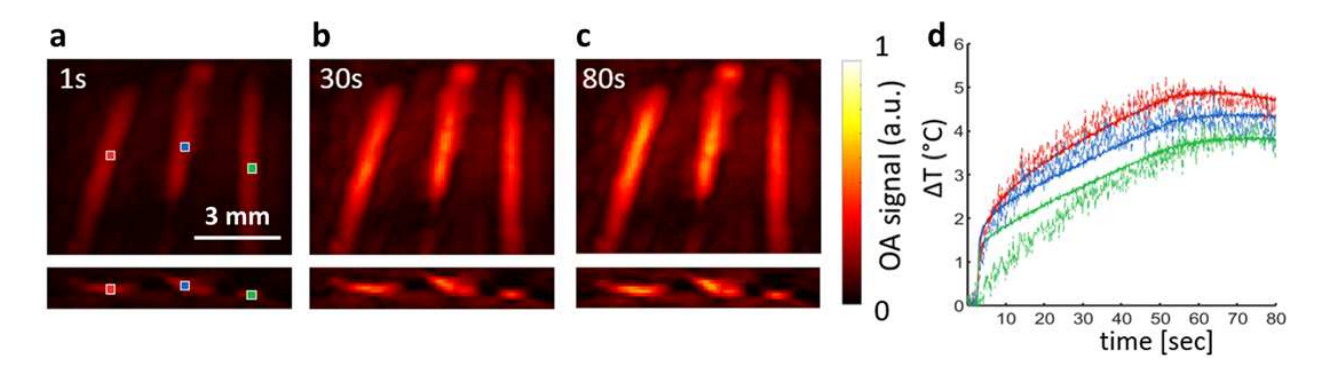


Figure 2. Optoacoustic temperature estimations in a tissue-mimicking phantom. (a)-(c) Transverse and coronal maximum intensity projection (MIP) optoacoustic images reconstructed for three different time points during laser heating of the phantom; (d) The temperature increase estimated from the optoacoustic signal variations (dashed curves) as compared to the temperature increase measured with thermocouples (solid curves). The regions of interest considered for the estimation are marked in panel (a).

As showcased, lower disagreement between the optoacoustically-estimated temperature values and those measured with the thermocouples results from higher temperature increments. This deviation can be partially attributed to the relative uncertainty in the measured  $\Delta p_0$  values (see Eq. 3), originating from the noise in optoacoustic measurements. Note however that the discrepancy may also result from inaccuracies in the theoretical F values that were calculated using Eq. 4 assuming a homogenous water medium. Further small uncertainties can be driven from the location of the thermocouple sensor tip.

Note also that in the experiments performed, the temperature dependence of the Grüneisen parameter was adopted from an empirical formula corresponding to diluted aqueous solutions, which may not accurately represent the physical reality in soft biological tissues.<sup>14</sup> Thus, accurate calibration of this parameter in different tissues may result in better accuracy when estimating the temperature-dependence of the OA signals. In addition, the accuracy of the temperature estimations has been shown to be directly linked to the contrast and noise levels of the reconstructed optoacoustic images while the average optoacoustic signal strength is expected to drop by approximately an order of magnitude for each centimeter of penetration in living tissues at near-infrared wavelengths.<sup>16,18</sup> At deep locations, one potential solution may involve guiding the optoacoustic excitation beam through the same fiber used for delivering the ablation beam.

The amount of monitored information can be enhanced by acquisition of multispectral optoacoustic tomography (MSOT) data.<sup>20</sup> Since MSOT enables identifying spectral variations in the imaged tissue, it may further enhance the performance of the temperature monitoring approach by recognizing alterations in optical parameters of the imaged tissue resulting from e.g. tissue coagulation.

In this work, we investigated the heating process with the assumption that optical properties remain unchanged due to coagulation or other irreversible thermal damage. The computation of the optoacoustic inversion and thermal diffusion models required for accurate temperature estimations from MSOT data becomes much more complex and wil be studied in future work.

During *in-vivo* thermal therapy procedures, it is further anticipated that blood perfusion will play a dominant role in thermal diffusion effects. Also, blood perfusion has a natural cooling effect  $^{21,22}$  that should have to be taken into account in order to accurately compute temperature in real-time during in-vivo investigations.

# 4. CONCLUSION

In conclusion, we establish a new high resolution volumetric temperature monitoring method during photothermal therapy based on real-time acquisition of three-dimensional optoacoustic data. This novel approach enables real-time estimation of the temperature fields during laser-induced thermotherapy procedures. The method suggested is expected to improve the safety and efficacy of thermal ablation treatments and to advance the general applicability of laser-based therapy.

### ACKNOWLEDGMENTS

The authors acknowledge support from the German Research Foundation (DFG) under Research Grant RA 1848/5-1.

#### REFERENCES

- 1. Moros, E.G. Physics of thermal therapy: fundamentals and clinical applications. CRC Press, (2012).
- 2. Chu, K.F. & Dupuy, D.E. Thermal ablation of tumours: biological mechanisms and advances in therapy. *Nature Reviews Cancer.* **14**, p. 199–470, (2014).
- 3. Torres-Reveron, J., Tomasiewicz, H.C., Shetty, A., Amankulor, N.M. & Chiang, V.L. Stereotactic laser induced thermotherapy (LITT): a novel treatment for brain lesions regrowing after radiosurgery. *Journal of neuro-oncology.* **113**, p. 495–503, (2013).
- 4. Oyaga Landa, F. J. et. al. Noncontact monitoring of incision depth in laser surgery with air-coupled ultrasound transducers. *Optics letters.* **41**, p. 2704–2707, (2016).
- 5. Datta, N. R. et. al. Local hyperthermia combined with radiotherapy and-/or chemotherapy: Recent advances and promises for the future. *Cancer Treatments Reviews.* **41**, p. 742–753, (2015).
- 6. Bandyopadhyay, S. et. al. Low-Intensity focused ultrasound induces reversal of tumor-induced T Cell tolerance and prevents immune escape. *The Journal of Immunology.* **196**, p. 1964–1976, (2016).
- 7. Shaw, A., Haar, G.T., Haller, J. & Wilkens, V. Towards a dosimetric framework for therapeutic ultrasound. *International Journal of Hyperthermia.* **31**(2), p. 182–192, (2015).
- 8. Gao, L. et. al. Single-cell photoacoustic thermometry. J. Biomed. Opt. 18(26003), (2013).
- 9. Deán-Ben, X.L. et. al. Advanced optoacoustic methods for multiscale imaging of in vivo dynamics. *Chemical Society Reviews.* **46**(8), p. 2158–2198, (2017).
- Pang, G.A., Bay, E., Deán-Ben, X.L. & Razansky, D. Three-dimensional optoacoustic monitoring of lesion formation in real time during radiofrequency catheter ablation. *Journal of cardiovascular electrophysiol*ogy. 26(3), p. 339–345, (2015).
- 11. Gray, J. et. al. Multi-wavelength photoacoustic visualization of high intensity focused ultrasound lesions. *Ultrason. Imaging.* **38**(3), p. 96–112, (2015).
- 12. Petrova, E.V., Motamedi, M., Oraevsky, A.A. & Ermilov, S.A. In vivo cryoablation of prostate tissue with temperature monitoring by optoacoustic imaging. *Proc. SPIE.* **9708**(97080G), (2016).
- 13. Fehm, T.F. et. al. Volumetric optoacoustic imaging feedback during endovenous laser therapy an ex vivo investigation. J. Biophotonics. 9, p. 934–941, (2015).
- 14. Oyaga Landa, F.J., Deán-Ben, X.L., Sroka, R. & Razansky, D. Volumetric optoacoustic temperature mapping in photothermal therapy. *Scientific Reports.* **7**(1), 9695, (2017).
- 15. Ozbek, A., Deán-Ben, X.L. & Razansky, D. Realtime parallel back-projection algorithm for three-dimensional optoacoustic imaging devices. *European Conference on Biomedical Optics.*, 88000I, (2013).
- 16. Wang, L.V. & Wu, H. Biomedical optics: principles and imaging. John Wiley & Sons. (2012).
- 17. Alexander A. Oraevsky, A.A., Esenaliev, R.O., Motamedi, M., Karabutov, A.A. Real time optoacoustic monitoring of changes in tissue properties. *US Patent* 6,309,352.
- 18. Deán-Ben, X.L., Fehm, T.F., Gostic, M. & Razansky, D. Volumetric hand-held optoacoustic angiography as a tool for real-time screening of dense breast. *Journal of Biophotonics*. **9**(3), p. 253–259, (2016).
- 19. Niemz, M.H. Laser-tissue interactions: fundamentals and applications. Springer Science & Businnes Media. (2013).
- 20. Deán-Ben, X.L. & Razansky, D. Functional optoacoustic human angiography with handheld video rate three dimensional scanner. *Photoacoustics*. **1**(3), p. 68–73, (2016).
- 21. Chu, K.F. & Dupuy, D.E. Thermal ablation of tumours: biological mechanisms and advances in therapy. *Nature Reviews Cancer.* **14**, p. 199-208, (2014).
- 22. Shih, T. et. al. Numerical analysis of coupled effects of pulsatile blood flow and thermal relaxation time during thermal therapy. *International Journal of Heat and Mass Transfer.* **55**, p. 3763–3773, (2012).